

**International Conference on
Geothermometry
and
Geobarometry**

— 1975 —

EXTENDED ABSTRACTS

International Conference on
Geothermometry and Geobarometry, 1975

The Pennsylvania State University

October 14-19, 1975

CONTENTS

Garnet Pyroxene Equilibria in the System CaSiO_3 - MgSiO_3 - Al_2O_3 & in a Natural Mineral Mixture	1
Geophysical Evidence on the Deep Structure of Continents & Associated Geodynamical Problems	5
Volcanic Temperature & Pressure Inferred from Inclusions in Phenocrysts	7
Pressure-Temperature History of the Mt. Albert Peridotite Intrusion & Its Implication for the Origin of Ultramafic Xenoliths in Basalts	11
Geothermometry & Geobarometry of the Earth's Mantle: An Analysis of Temperature Distribution of the Man- tle Based on the Electrical Properties of Minerals at High Pressure	13
Quantitative Regional Geobarometry of the Anorthositic Nain Complex, Labrador	15
Anion Distribution Among Coexisting Minerals of Grenville Marbles	19
Fe-Ni Partition in Metamorphosed Olivine-Sulfide Assemblages from Perseverance, Western Australia	21
Garnet Granulites of the Adirondacks	23
Application of Thermometry to Contact Metamorphism at Elkhorn, Montana	25
Chemical Inhomogeneities in Minerals in Kimberlite Nodules from Lesotho & the Kimberley Pipes	27
Margarite Stability & Compatibility Relations in the System CaO - Al_2O_3 - SiO_2 - H_2O as a Pressure-Temperature Indicator	31
Oxygen Isotope Geothermometry, A Review	35
Partial Melting in the Josephine Peridotite & Its Consequence for Pyroxene Geobarometry & Thermometry ..	39
Pyroxenes of the Ronda Peridotite	43
Plagioclase Thermometry & Barometry in Igneous Systems ..	45
Electrical Conductivity & the Geotherm	49
The Solubility of Al_2O_3 in Orthopyroxenes in Spinel & Plagioclase Peridotites & Spinel Pyroxenite	53
A Field Test of Geothermometers & Barometers	55
Downhole Fission Track - $^{40}\text{K}/^{40}\text{Ar}$ Age Determinations & the Measurement of Perturbations in the Geothermal Gradient	59

Limits to the Assemblage Forsterite + Anorthite as Inferred from Peridotite Hornfelses, Icicle Creek, Washington	63
Intracrystalline Cation Distribution in Aluminous Orthopyroxene, & Its Implications	67
Plagioclase-Garnet- Al_2SiO_5 -Quartz: A Potential Geobarometer-Geothermometer	69
Alkali Exchange between Hornblende & Melt: A Tem- perature-Sensitive Reaction	73
Clinopyroxene Geothermometry of Spinel-Lherzolites	77
Discrepancies in the Apparent Solubility of Al_2O_3 in Enstatite at High Pressure	79
On Deducing Paleogeotherms from Xenolith Suites in Basalts & Kimberlites: A Heisenbergian Uncertainty ...	83
High Temperature Contact Metamorphism of Carbonate Rocks in a Shallow Crustal Environment, Christmas Mountains, Big Bend Region, Texas	87
Comparison of Methods for Calculating & Extrapolating Equilibria in P-T- X_{CO_2} Space	91
Magma Ascent in Island Arcs	93
The Equilibrium Fe^{2+} -Mg Distribution in Ca-Rich Clinopyroxenes	97
Single Pyroxene Geothermometry & Geobarometry. Application to Some Geological Problems	101
Experimental Studies of Pyroxenes at High Pressures	105
High-Al Pyroxene in Anorthosite: Barometer or Speedo- meter	109
Experimentally Determined Pressure, Temperature, & Chemical Variables in Peridotites to 30 Kbar: Geothermometry & Geobarometry	111
Calculation of Ultramafic, Spinel-Bearing Mineral Assemblages at Different Pressures & Temperatures	117
Thermochemistry of Some Diopsidic Pyroxenes; Implica- tions for Distribution Coefficients & for the Pyroxene Geotherm	121
Pyroxene Grids, Palaeogeotherms & a New Mineral Facies in the Upper Mantle	123
Pressure Required to Stabilize Garnet-Peridotite & Eclogite at Low Temperatures	127
Great Thickness & High Geothermal Gradient of Archaean Crust: The Lewisian of Scotland	131

Variation in Geothermometry & Geobarometry of Peridotite Intrusions in the Dinaride Central Ophiolite Zone, Yugoslavia	133
Chromium-Rich Pyroxenes of Megacrysts & Peridotite Xenoliths in Basalt, Black Rock Summit, Nevada	137
A Nepheline-Alkali Feldspar Geothermometer	141
Temperature, Pressure & Fluid Phase Composition for the Formation of a Graphitic Calc-Pelite	145
Alumina Content of Enstatite as a Geobarometer for Spinel Lherzolites	147
The Orthoclase-Microcline Inversion in Metamorphic Rocks of the Western Hohe Tauern (Eastern Alps)	149
Experimental Calibration of the K_D^{Ga+cpx} -Geothermometer & Its Application on Eclogitic Rocks	153
Petrologic Constraints on the Hawaiian Geotherm	157
Petrologic Data from Experimental Studies on Crystal- lized Silicate Melt & Other Inclusions in Olivine	161
Clinopyroxene Exsolution Lamellae: Fossil Indicators of Lattice Parameters at High Temperature & Pressure	165
Oxygen Fugacity Geothermometry: Part I. Reliability of Equipment	169
A Pyroxene Geothermometer Based on Composition- Temperature Relationships of Naturally Occurring Orthopyroxene, Pigeonite, & Augite	173
Polymorphic Phase Boundaries & Lateral Heterogeneity in the Upper Mantle	177
Electrochemical Geothermometry - Current Status & Future Possibilities	179
Pressures of Formation of Some Meteorites from Sphalerite Compositions	183
Relationship of a High-Pressure Oxonium Mica in the System $MgO-SiO_2-H_2O$ to Thermal Models of Descending Lithospheric Slabs	187
Sulfide Geothermometers & Geobarometers	191
Thermal Regimes in Cratered Terrain with Emphasis on the Role of Impact Melt	197
APL Computer Programs for Thermodynamic Calculations of Equilibria in P-T- X_{CO_2} Space	201
Geophysical Constraints on Radial & Lateral Temperature Variations in the Upper Mantle	203
Volatiles in Quartz: A Potential Method of Geobarometry..	207

Intracrystalline Distributions in Geothermometry & Geobarometry	211
Cation-Exchange Thermometry in Metamorphic Rocks	213
Garnet Composition & Zoning in the Determination of Temperature & Pressure of Metamorphism, Central Massachusetts	215
Oxygen Fugacity Geothermometry: Part II. Petrogenetic Case Histories	219
Geothermometry & Geobarometry in Epizonal Granitic Intrusions: A Comparison of Iron-Titanium Oxides & Coexisting Feldspars	223
An Experimental Study of the Effects of Heat Removal on the Phase Relations of Basaltic Systems	227
Mixing Properties of Tschermakitite Clinopyroxenes & Their Application to Geobarometry	231
Petrogenetic Grid for Siliceous Dolomites Extended to Mantle Peridotite Compositions, & to Conditions for Magma Generation	235

GARNET PYROXENE EQUILIBRIA IN THE SYSTEM CaSiO_3 - MgSiO_3 - Al_2O_3 AND IN A NATURAL MINERAL MIXTURE

Jagannadham Akella (TN7, NASA Johnson Space Center, Houston, TX 77058)

Experimental phase equilibria studies can be used in estimating the P and T conditions of equilibration of the ultramafic xenoliths, provided the original equilibria established at depth in the upper mantle were preserved undisturbed during eruption. There are compositional variables among the minerals present in the ultramafic nodules that are sensitive functions of pressure and temperature. The conditions of formation can be estimated, therefore, by equilibrating natural rock samples or mineral mixtures at known conditions, and by studying the compositional variables in the minerals of simple synthetic systems which approximately model those in these rocks.

The ternary system CaSiO_3 - MgSiO_3 - Al_2O_3 encompasses the garnet join $\text{Ca}_3\text{Al}_2\text{Si}_3\text{O}_{12}$ - $\text{Mg}_3\text{Al}_2\text{Si}_3\text{O}_{12}$ and the pyroxene join $\text{CaMgSi}_2\text{O}_6$ - MgSiO_3 and also illustrates the solid solutions between them. At high pressures this system contains a three phase field, enstatite-diopside-garnet, which is invariant at constant pressure and temperature (Boyd, 1970). The compositional coordinates of this three phase field as a function of pressure and temperature form an important basis for estimation of the equilibration pressures and temperatures of natural garnet peridotites.

The set objectives in the present study were: a) to check the usefulness of the $\text{Ca}/(\text{Ca}+\text{Mg})$ ratio of orthopyroxene coexisting with clinopyroxene and garnet, as a geothermometer, b) to determine the solubility of Al_2O_3 in the orthopyroxene coexisting with garnet and clinopyroxene as a function of pressure and temperature in the system CaSiO_3 - MgSiO_3 - Al_2O_3 , c) to determine the influence of Ti and Fe on the solubility of Al_2O_3 in the orthopyroxene and d) to compute and compare the equilibration pressures estimated for experimentally equilibrated natural mineral mixtures, using the phase data for MgSiO_3 - Al_2O_3 (McGregor, 1974), MgSiO_3 - CaSiO_3 - Al_2O_3 (present study) and Wood's (1974) thermodynamic model.

Compositions on the pyrope-diopside join in the CaSiO_3 - MgSiO_3 - Al_2O_3 ternary system were investigated between 26-44 kbar and 1000-1500°C. Two bulk compositions were utilized in this study; one with pyrope₇₅-diopside₂₅ and a second composition pyrope₇₀-diopside₃₀, to which 5 wt. % $\text{CaTiAl}_2\text{O}_6$ was added to test the effect of Ti on the solubility of alumina in the orthopyroxene. The subsolidus phase assemblage for these compositions is garnet + clinopyroxene + orthopyroxene. Chemical composition of the coexisting phases in the experimental products were determined using electron microprobe.

Boyd and Nixon (1973) have suggested that the $\text{Ca}/(\text{Ca}+\text{Mg})$ ratio of enstatite in equilibrium with diopside is a potential geothermometer. The $\text{Ca}/(\text{Ca}+\text{Mg})$ ratio of enstatites from the present experiments are plotted as a function of temperature along with Boyd and Nixon's empirical "enstatite thermometer", Fig. 1. Present results suggest

that this ratio decreases with pressure. A comparison of the present data with the data obtained by Mysen and Boettcher (1974) at pressures in the 7.5-15 kbar range strongly supports this concept of pressure effect.

Solubility of Al_2O_3 in the orthopyroxene coexisting with garnet + clino-pyroxene decreases as pressure increases and as temperature decreases. The form of isopleths obtained for the present ternary system is very similar to that obtained for the binary join MgSiO_3 - Al_2O_3 . The presence of small amounts of TiO_2 in the bulk composition does not have marked effect on the solubility of Al_2O_3 in pyroxenes. The first significant drop in the Al_2O_3 content of the orthopyroxene occurs in the system where FeO was added, Table 1. However, the alumina solubility in orthopyroxenes determined in the Fe-bearing system are nearly the same as those for the natural mineral mixtures equilibrated at the same P and T conditions.

Using the chemical composition of the experimentally equilibrated garnets and pyroxenes, equilibration pressures and temperatures are indirectly estimated on the basis of direct application of phase data for MgSiO_3 - Al_2O_3 (EnCo) and CaSiO_3 - MgSiO_3 - Al_2O_3 (WoEnCo) systems and Wood's model, Table 2. Equilibration pressures estimated on the basis of direct application of phase data for both WoEnCo and EnCo, are all higher than the measured equilibration pressures. Wood's thermodynamic model works well for the results at 31 kbar, but corrections obtained for runs at 38 and 44 kbar are in the 4-5 kbar range.

References

- BOYD, F. R. (1970) Garnet peridotites and the system CaSiO_3 - MgSiO_3 - Al_2O_3 . Mineral. Soc. Am. Spec. Pap. 3, 63-75.
- _____, AND P. H. NIXON (1973) Origin of the ilmenite-silicate nodules in kimberlites from Lesotho and South Africa. In, P. H. Nixon, Ed., Lesotho Kimberlites, Lesotho National Development Corporation, Maseru, Lesotho, 254-268.
- MAC GREGOR, I. D. (1974) The system MgO - Al_2O_3 - SiO_2 : Solubility of Al_2O_3 in enstatite for spinel and garnet peridotite compositions. Am. Mineral. 59, 110-119.
- MYSEN, B. O., AND A. L. BOETTCHER (1974) Melting in a hydrous mantle, II, Geochemistry of crystals and liquids formed by anatexis of mantle peridotite with controlled activities of H_2O , CO_2 and O_2 . J. Petrol. (In press).
- WOOD, B. J. (1974) Solubility of Al_2O_3 in orthopyroxene coexisting with garnet. Contrib. Mineral. Petrol. 46, 1-15.

TABLE 2. Experimental and Calculated* Equilibrium Temperatures and Pressures for a Natural Enstatite+Diopside+Garnet Assemblage

Run No.	Al ₂ O ₃ in En	Temp., °C		Pressure, Kbar			
		Exp.	Calc.	Exp.	EnCo	WoEnCo	Wood
N-7	3.54	1300	1285	31	40	38	31
N-10	2.43	1300	1325	44	47	45	40
N-8	2.48	1100	1145	31	35	37	29
N-13	1.69	1100	1040	38	42	43	33

*Temperature calculated from Ca/(Ca+Mg) using the diopside solvus (Boyd, 1973). Pressure calculation: EnCo, from MgSiO₃-Al₂O₃ (MacGregor, 1974); WoEnCo, from CaSiO₃-MgSiO₃-Al₂O₃ (Akella, this Report); Wood, from a theoretical relation described by Wood (1974). The measured temperature was used in the pressure calculations.

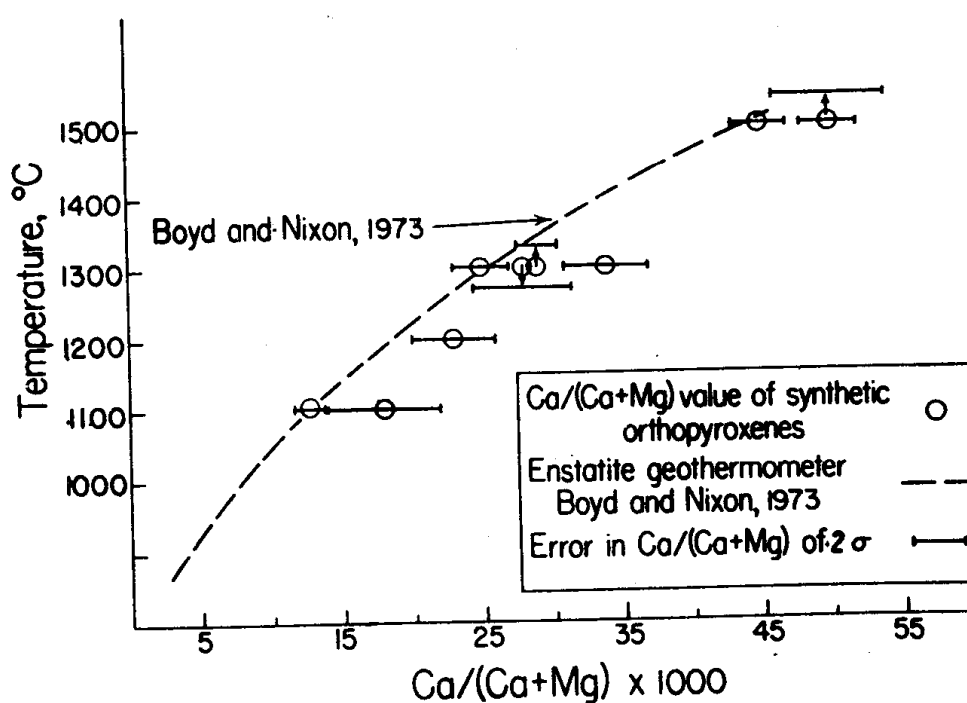


Fig. 1. The Ca/(Ca+Mg) ratios of orthopyroxene coexisting with clinopyroxene and garnet at different pressures as a function of temperature. Dashed line is an "empirical curve" for enstatite in ultramafic nodules given by Boyd and Nixon (1973).

Table 1. Solubility of Al_2O_3 (wt. %) in orthopyroxene coexisting with garnet and clinopyroxene at 31 and 44-Kbar pressure and 1100°C in different systems.

			31 Kbar/1100°C		
	$\text{MgSiO}_3\text{-Al}_2\text{O}_3^+$	$\text{CaSiO}_3\text{-MgSiO}_3\text{-Al}_2\text{O}_3$	$\text{CaSiO}_3\text{-MgSiO}_3\text{-CaTiAl}_2\text{O}_6$	$\text{CaSiO}_3\text{-MgSiO}_3^{**}$ $\text{FeSiO}_3\text{-CaTiAl}_2\text{O}_6$	Naturals*
Al_2O_3	3.3	3.1	3.1	2.6	2.5
			44 Kbar/1100°C		
Al_2O_3	[1.5]	1.6	1.6	1.4	1.39

+ McGregor, 1974.

* Akella and Boyd, 1974.

** Akella and Boyd, 1973.

[] Extrapolated value.

GEOPHYSICAL EVIDENCE ON THE DEEP STRUCTURE OF CONTINENTS AND ASSOCIATED GEODYNAMICAL PROBLEMS

S. S. Alexander (Dept. of Geosciences, The Pennsylvania State Univ., University Park, Pa. 16802)

Consideration of a variety of geophysical observations for different shields reveals that the mantle structure beneath shields is everywhere remarkably similar but distinctly different from the structure beneath intervening ocean basins to depths of the order of the 400 km or 650 km seismic discontinuities. In sharp contrast to oceanic and active tectonic regions shields are characterized by the absence or near-absence of a mantle low-velocity zone, high Q , low temperature, low electrical conductivity, low seismicity, low absolute plate velocity, and lateral uniformity. The principal inference is that shields have moved about essentially as rigid units over depth extents of 400 km or more and may be compositionally different from younger oceanic mantle; in turn this implies significant motion and lateral variations of physical properties deeper in the mantle, as well as a different pattern of shallow mantle motions beneath shields and ocean basins. The 400 km and 650 km seismic discontinuities may be important decoupling zones due to accelerated creep at solid-solid phase transitions.

VOLCANIC TEMPERATURE AND PRESSURE INFERRED FROM INCLUSIONS IN PHENOCRYSTS

A. T. Anderson (Dept. Geophysical Sciences, Univ. of Chicago, Chicago, Illinois 60637)

J. R. Sans (Dept. of Geophysical Sciences, Univ. of Chicago, Chicago, Illinois 60637)

The ratio of MgO in host pyroxene or olivine to that in included glass (D) is a sensitive indicator of temperature. We have repeated the study of Roeder (1974) on olivine-liquid partitioning of MgO by heating (at 1360, 1283, 1210, 1115 and 1068°C) natural crystals of olivine with inclusions of glass in evacuated SiO₂-glass vials and analyzing with the microprobe the quenched products. Our results are summarized on Fig. 1. The contours on Fig. 1 are for different values of a composition parameter equated by Roeder to the activity coefficient of FeO in melt. The parameter is presumed to relate similarly to the activity coefficient of MgO. The parameter accounts for about 70 percent of the variation in the distribution factor at a fixed temperature and reduces the probable error in the estimated temperature from about 60°C to about 20°C. For the same distribution of MgO, our temperatures are 20 to 40°C higher than Roeder's, possibly because of our error in temperature measurement. As novice experimentalists using a novel technique, we are gratified by the close agreement of our results with Roeder's.

We extended the experimental calibration to orthopyroxene and glass by using the same technique. The results are shown on Fig. 2 and are based on data at 1210, 1115 and 1068°C. Glasses included in pyroxene phenocrysts are generally andesitic to rhyolitic in composition. This fact, together with the lower temperature, raises the question of equilibrium attainment. Results obtained at 1068°C (200 hrs) are plotted on Fig. 3 together with analyses of natural (unheated) glasses. Similar starting materials with both higher and lower initial D (S76 and S17) yielded similar results. SiO₂ (rather than the composition parameter) gives a good correlation with D and accounts for most of the isothermal variation. With rare exception analyses of natural and heated glasses define an SiO₂ correlation with distribution factor which is consistent with a precision of ±40°C in estimated temperature (above 1000°C) for an individual inclusion.

Applied to natural materials, the calibrations of Figs. 1 and 2 yield estimates of temperature which are broadly consistent with other data. For Kilauea the temperature of extrusion inferred from glasses in olivine and pyroxene are within error of each other and of pyrometer readings on lava fountains. Also, the estimated temperature of intratelluric crystallization after allowing for 1 weight percent of H₂O (suggested by comparison with submarine lavas) in the light of Eggler's (1972) data is in accord with estimates based on Fe-Ti oxide phenocrysts. For Paricutin and Pacaya the range of temperatures is consistent with pyrometer observations, but there is room for improvement.

The temperature of crystallization of phenocrysts (T_p) is more important than the temperature of extrusion. An upper limit to T_p can be inferred by reconstructing the composition of the melt from which the phenocrysts grew. After melt is entrapped (and perhaps before) its composition is modified by crystallization or resolution of the host crystal.

Since crystallization of pyroxene depletes the melt in MgO and plagioclase enriches it in MgO, inclusions of glass in coprecipitated pyroxene and plagioclase suffice to establish the composition of the initial melt. Values of T_p reported in Table 1 are arrived at in the above manner. The important result is that all andesitic melts so far encountered have crystallization temperatures below 1100°C. The more silicic the melts, the lower the temperature. There is no support for the low temperature "andesite trough" proposed by some Australian scientists.

The upper temperature limit, T_p , should be decreased in accord with the concentration of H₂O in the melt. We have estimated the latter by difference and arrived at a decreased temperature (T^*) on the basis of the results of Eggler (1972). The difference estimates of the concentrations of H₂O are consistent with evidence of loss of Cl relative to K₂O and with enlarged vapor bubbles in heated inclusions of glass which become surrounded by haloes of darkened (? oxidized) pyroxene or olivine. Vapor saturation is indicated by the presence of inclusions of vapor in phenocrysts and by the Cl/K₂O relation for glasses included in phenocrysts. The modified temperatures (T^*) are 100 to 200°C lower than temperatures inferred from analyses of magnetite and ilmenite phenocrysts, except for Kilauea where agreement is good. However, the low temperatures and high concentrations of H₂O do agree qualitatively with the presence of amphibole as phenocryst and with liquidus pyroxene for S76. T^* is commonly about 100°C lower than the extrusion temperature. This is possible because of mixing with hot basaltic magma before ascent and adiabatic crystallization and frictional heating during ascent.

A lapillus by lapillus dissection of stages of the 1783 eruption of Asama reveals (Fig. 3) that individual pumice lumps (11-13 = lumps from early phase, 21-23 from mid-phase; 31-33 from late phase) contain contributions from hot (andesitic and basaltic) sources and cold rhyolitic sources. The olivine crystals contain inclusions of andesitic glass exceptionally rich in Al₂O₃ (up to 22 weight percent) and with daughter crystals of spinel and rare hornblende. The occurrence of hornblende daughter crystal is consistent with the inferred extrusion temperature of 900-1010°C and the concentration of H₂O inferred by difference (4 weight percent) and experimentally determined stabilities of hornblende in andesitic and basaltic melts. The coldest material is found mainly in the material from the early part of the eruption.

Variable compositions and apparent temperatures of extrusion and initial crystallization (T_p) exist in most other andesitic tephra and suggest that in general andesites are assembled from variously solid parts of reservoirs of magma which range in pressure from about 500 atmospheres to more than 5000 atmosphere in rare cases, in temperatures from about 1200°C to 700°C but mostly in the 900 to 1100°C interval, and which are commonly saturated with vapor, particularly in crystal-rich regions.

References:

- Eggler, D. H. (1972) Water-saturated and undersaturated melting relations in a Paricutin andesite and an estimate of water content in the natural magma. Contrib. Mineral. Petrol. 34, 261-271.
Roeder, P. L. (1974) Activity of iron and olivine solubility in basaltic liquids. Earth Planetary Sci. Lett. 23, 397-410.

TABLE 1. TEMPERATURES OF CIRCUMPACIFIC TEPHRA

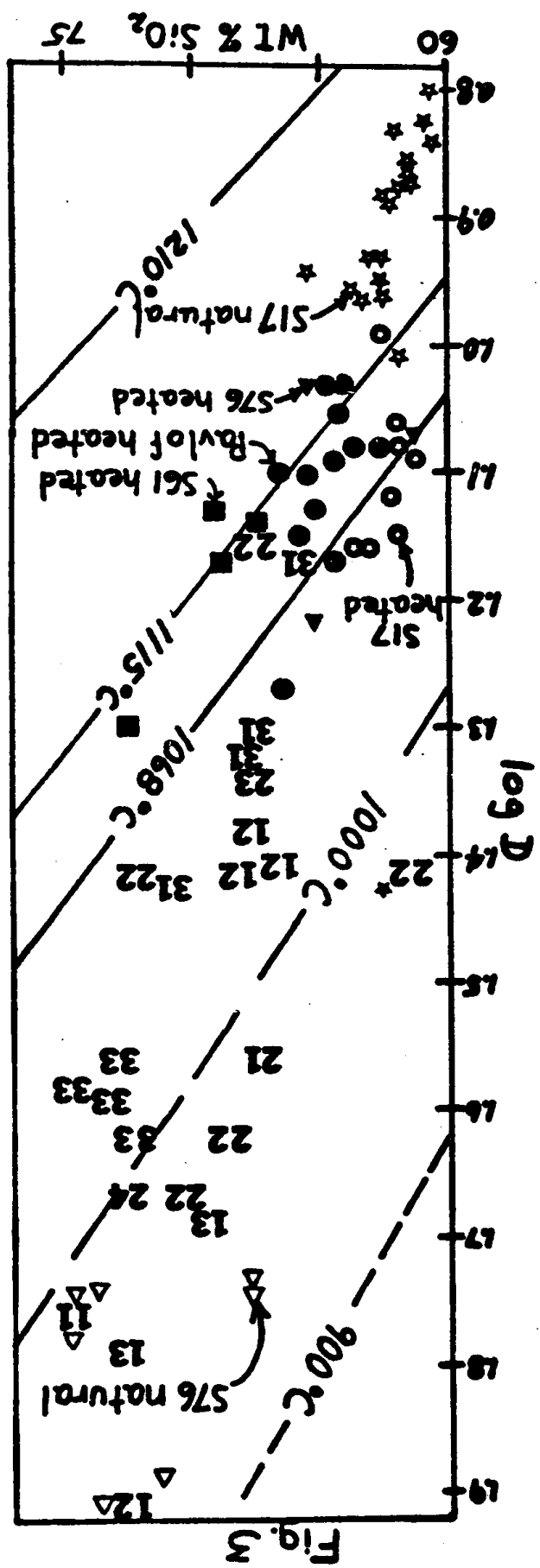
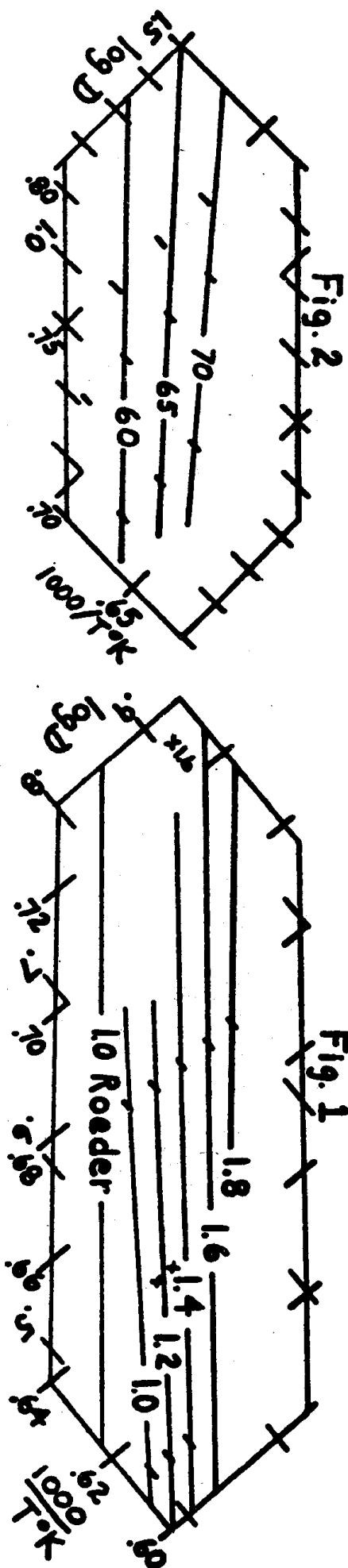
Volcano	Eruption	T _{px} ¹	T _{ol} ²	T _p ³	H ₂ O _p ⁴	T* ⁵	T _{other}	Note ⁸	SiO ₂ ⁹
Arenal	1968	1010		1080	7	900		P1, Px, O1, Hb	63
Asama	1783	960-1050		980	4	860	1000-1070 ⁶	En65, An65	72
Asama	1783	980-1060			4			En73-69	65
Asama	1783		900-1010		1-4			Fo85-79	55-61
Goosenest	S73		1090						52
Goosenest	S74		980						57
Kilauea	1955	1100	1140	1160	1	1120	1060-1180 ^{6,7}		51
Pacaya	1975		1060	1220	3	1120	1040-1130		51
Pavlof	Cone G	1050	1010	1030	3	930			63
Pavlof	1973	1100					"yellow" fires	P1, Px	58
Paricutin	1944-1948		870-1100				1070-1130 ⁷	P1, Px, O1	54-62
Shasta	S17		1090		6				56
Shasta	S17	1140	1020		1			Px, O1, (P1)	62
Shasta	S41	920		920	5	770	860-1070 ⁶	P1, Px, O1, Hb	76
Shasta	S61	1000		1010	3	910	1040-1110 ⁶	P1, Px, O1	72
Shasta	S76	950		1100	12	900		En85, Di83, (Hb)	67

^{1,2}Temperatures inferred from D on the basis of calibrations presented in Figs. 1 and 2 for pyroxene and olivine respectively. ³Inferred temperature of crystallization of phenocrysts (see text).

⁴Inferred concentrations of H₂O in melt from which phenocrysts grew. ⁵T_p adjusted to take account of H₂O_p.

^{6,7}Temperatures inferred from compositions of Fe-Ti oxide phenocrysts and from optical pyrometer measurements of erupting lava. ⁸Petrographic data giving nature and/or compositions of phenocryst minerals.

Parentheses denotes past presence inferred from breakdown products. ⁹The weight percent of SiO₂ (anhydrous basis) characteristic of the glass on which either T_p or T* are based (T_{px} or T_{ol} is no data for T_p or T*). The whole rocks are generally less silicic than the glasses associated with pyroxene but commonly are more silicic than the glasses associated with olivine.



PRESSURE-TEMPERATURE HISTORY OF THE MT. ALBERT PERIDOTITE INTRUSION
AND ITS IMPLICATION FOR THE ORIGIN OF ULTRAMAFIC XENOLITHS IN BASALTS

Asish R. Basu (Dept. of Geology and Geophysics, University of Minnesota,
Minneapolis, Minnesota 55455)

Ian D. MacGregor (Dept. of Geology, University of California, Davis,
California 95616)

Recent evidence from ultramafic xenoliths in alkali basalts and kimberlites suggest that diapiric upwelling in the upper mantle is an important event prior to the generation of magma. The high temperature peridotite body of Mt. Albert in eastern Canada provides a good example, to examine in detail, a cross-section of such a diapiric intrusion (MacGregor and Basu, in preparation).

Two hundred and twenty samples of harzburgites and spinel lherzolites from various parts of the intrusion were analyzed for their coexisting mineral phases. The major element chemistry of olivine, orthopyroxene, clinopyroxene and spinel have been used to estimate pressure and temperature of equilibration of various mineral pairs. The diopside-enstatite solvus shows temperatures of equilibration in the range 850°C-1000°C. Olivine-spinel pair indicates a much greater range, from 850°C-1300°C. The Cr-Al distribution coefficients of coexisting pyroxenes (Mysen and Boettcher, 1975) show a range of temperatures between 850°C to 1200°C. The empirical data of Mysen and Boettcher give results that yield credible temperatures because the data are shown to be independent of pressure and based on experiments of comparable composition. Pressures of equilibration from the alumina content of the coexisting orthopyroxenes (MacGregor, 1974) show pressure variations from 12-28kbs, 12-40kbs and 12-32kbs in conjunction with the diopside-enstatite, olivine-spinel and the Cr-Al-partitioning-coefficient-between-pyroxenes thermometers, respectively. Samples with high chrome-alumina ratios in spinel suggest abnormally high pressures of equilibration. When an empirical correction is applied for the effect of high chromium in spinel, all the Mt. Albert peridotites show a linear relationship in pressure-temperature space.

Texturally, the peridotite body shows systematic variation with coarse grained, undeformed granular texture in the center of the body. This texture grades outward into a porphyroclastic texture, followed successively by fine grained equigranular tabular and mosaic texture at the margin of the body. The variation in texture is accompanied by drastic reductions in the average grain size of the rocks. Moreover, the least deformed rocks are most lherzolitic (diopside rich) while the most deformed rocks are most refractory (harzburgitic). The more deformed rocks around the margin show equilibration at lower temperatures and pressures while the less deformed rocks of the core of the intrusion retain higher relict temperatures and pressures.

All the four textural types found in the Mt. Albert peridotite body and reported from world-wide occurrences of ultramafic xenoliths in basalts (Mercier and Nicolas, 1975) are also present, with some modification, in the ultramafic xenoliths from San Quintin, Baja California. Similar to the Mt. Albert peridotites, the equigranular and the tabular mosaic textures in these xenoliths also show equilibration at lower

//